

Power Spectra of Fluctuations in Strong Langmuir Turbulence

D. F. DuBois, Harvey A. Rose, and David Russell

Theoretical Division, Los Alamos National Laboratory, Los Alamos, New Mexico 87545

(Received 6 July 1988)

The power spectral densities of turbulent fluctuations computed from Zakharov's model are shown to have unexpected structure which results from the coherent temporal evolution of cavitons. These spectra have features in common with the spectra measured during ionospheric heating.

PACS numbers: 52.35.Ra, 03.40.Kf

Recently¹ we presented the first calculations of the power spectrum, $\langle |\mathbf{E}(\mathbf{k}, \omega)|^2 \rangle$, of electric field (envelope) fluctuations in the Zakharov model² of strong Langmuir turbulence which showed that under conditions of strong to moderate ion-sound-wave damping a major part of the spectral energy was contained in localized states. In most applications, and in particular for ionospheric heating experiments,³ the putative driving-field intensities are in the strong turbulence regime. It is then essential to understand how the observed spectra are explained by strong turbulence theory.⁴

In this Letter we investigate the surprisingly detailed power spectra observed in computer solutions of the Zakharov model and try to determine what can be learned from these spectra about the dynamics of strong Langmuir turbulence. Again our simulations are based on the Zakharov² model:

$$\nabla \cdot [i \partial_t \mathbf{E} + i v_e \circ \mathbf{E} + \nabla^2 \mathbf{E} - n \mathbf{E}] = \mathbf{E}_0 \cdot \nabla n, \quad (1a)$$

$$(\partial_t^2 n + 2 v_i \circ \partial_t n - \nabla^2 n) = \nabla^2 |\mathbf{E}_0 + \mathbf{E}|^2. \quad (1b)$$

We have used standard dimensionless variables^{5,6} and have decomposed the total envelope field into its spatially uniform part, $\mathbf{E}_0(t) = \mathbf{E}_0 \exp(-i\omega_0 t)$, which we take to be an imposed drive field—e.g., the ordinary mode of the rf ionosphere heater³—and the nonuniform longitudinal field $\mathbf{E}(\mathbf{x}, t)$. The dissipation operators v_e and v_i which are local in \mathbf{k} space and the numerical methods of solution are discussed in Ref. 1.

The present study was motivated by the observations of electric field power spectra, $|\mathbf{E}(\mathbf{k}, \omega)|^2$, from *single-caviton-collapse* events in weakly driven, two-dimensional simulations¹ in which only one caviton at a time is present in the simulation box.⁷ Spectra for two values of the wave vector are shown in Fig. 1 and have three qualitatively important features: (1) Essentially all the spectral energy occurs for $\omega < \omega_0 (=0)$ ⁸; (2) there are well-defined peaks in the spectrum; and (3) for increasing k the spectrum broadens and the peaks in the spectrum for more negative ω become relatively more important. These spectra and those of Ref. 1 are similar to the incoherent scatter radar spectra at early times in low-duty-cycle experiment.⁹ We would like to understand what properties of the caviton evolution are

reflected in these spectra of isolated cavitons and how these isolated-event spectra relate to a multicaviton system. To study the time evolution of an isolated event as it evolves from nucleation⁶ to collapse to burnout we have found it useful as in earlier work⁶ to resolve $\mathbf{E}(\mathbf{x}, t)$ in terms of a complete orthonormal set of *time-dependent* vector eigenfunctions $\mathbf{e}_v(\mathbf{x}, t)$, with eigenvalues $\lambda_v(t)$, associated with the instantaneous density perturbation $n(\mathbf{x}, t)$. These satisfy the equation

$$\nabla \cdot [\lambda_v(t) + \nabla^2 - n(\mathbf{x}, t)] \mathbf{e}_v(\mathbf{x}, t) = 0, \quad (2)$$

with $\nabla \times \mathbf{e}_v = 0$ and $\int d^3x \mathbf{e}_v^* \cdot \mathbf{e}_v = \delta_{vv}$. We then can write $\mathbf{E}(\mathbf{x}, t) = \sum_v h_v(t) \mathbf{e}_v(\mathbf{x}, t)$ where the sum may include an integral over continuum states. In a large system (such as the ionosphere) with many cavitons, there are states localized at a given site, say $\mathbf{e}_0(\mathbf{x}, t)$ localized at $\mathbf{x} = 0$, which asymptotically describe the collapse at that site. Since $n(\mathbf{x}, t)$ depends implicitly on $|\mathbf{E}|^2$, this may be viewed as a kind of nonlinear eigenvalue problem which goes over to the usual self-similar analysis of collapse.¹⁰ If $\lambda_0 < 0$, the amplitude $h_0(t)$ of this state evolves continuously from the nucleation stage to collapse.⁸ On

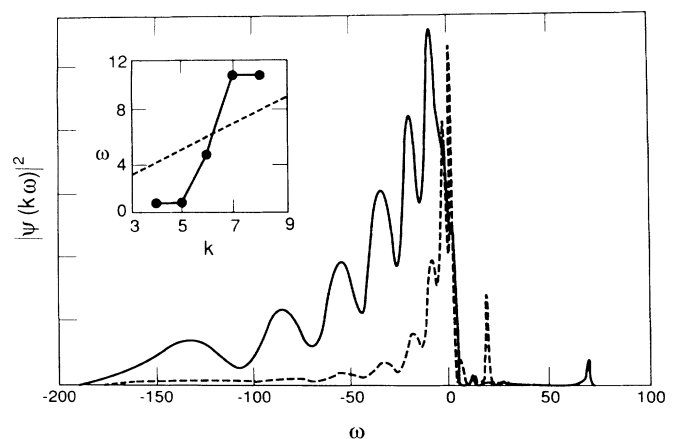


FIG. 1. Spectra, $|\Psi(\mathbf{k}, \omega)|^2 = k^{-2} |\mathbf{E}(\mathbf{k}, \omega)|^2$, for $D=2$ isolated collapse events. $E_0=0.8$, $v_i=0.9|\mathbf{k}|$, $m_i/m_e=1836$, $\omega_0=0$; dashed curve, $k_x=4$, $k_y=0$, and solid curve, $k_x=8$, $k_y=0$. Inset: Solid line, negative frequency at maximum of spectrum vs $k=k_x$; dashed line, ion acoustic shift, $|\omega|=k$.

substituting this expansion in Eq. (1a) it follows that the amplitudes $h_\nu(t)$ are coupled because of the time dependence of $n(\mathbf{x}, t)$. For h_ν we have, neglecting dissipation,

$$i\dot{h}_\nu - \lambda_\nu(t)h_\nu = S_\nu - i \sum_{\nu'} \int d\mathbf{x} \mathbf{e}_\nu^*(\mathbf{x}, t) \cdot \dot{\mathbf{e}}_{\nu'}(\mathbf{x}, t) h_{\nu'}(t), \quad (3)$$

where $S_\nu = \int d^3x \mathbf{E}_0 \cdot \mathbf{e}_\nu^*(\mathbf{x}, t) n(\mathbf{x}, t)$ and overhead dots denote time derivatives. Note that the amplitude for a state ν is driven directly by the pump and is coupled to other states ν' as a result of the time dependence of the eigenstates which derives directly from the time dependence of $n(\mathbf{x}, t)$. Nonlocalized modes are excited through this mechanism by the strongly time-dependent density cavities resulting from the collapse of localized states. Such nonlocalized modes show up as relatively weak features in the spectra near the free Langmuir wave frequency $\omega \sim k^2$ in Fig. 1 and in the spectra of Fig. 3 of Ref. 1, but are relatively stronger during the onset of turbulence. Despite the name which we gave to these features in Ref. 1, they are *not* predicted by standard weak-turbulence arguments.

We have gained useful insight into the nucleation-to-collapse evolution and its connection with the power spectra by considering the *scalar*^{11,12} Zakharov equations in which only spherically symmetric collapsing cavitons are allowed and the three-dimensional problem for an isolated collapse reduces to one in which $E(r, t)$ and $n(r, t)$ depend only on the radial coordinate r . This scalar model has several properties in common with the physical *three-dimensional* vector model of Eq. (1): threshold and maximum growth rate for the modulational instability, collapse scaling exponents, no threshold energy for collapse, and the failure of a density well to always support a localized eigenstate.

Spherical symmetry is imposed by our representing all

fields in terms of the Fourier modes $\sin(k_l r)$, $k_l = \pi l / r_0$, $l = 1, 2, \dots$, with r_0 chosen large compared to a typical caviton size. In these scalar studies we have observed for $v_i(k)/k = 0.9$ that at the nucleation site, $E(r, t)$ is dominated by its projection, $h_0(t)$, on the localized ground state $e_0(r, t)$. In nucleation $e_0(r, t)$ remains localized; at every time step $e_0(r, t)$ can be computed from $n(r, t)$. Here we will adopt a simplified model in which $h_0(t)$ is evolved with neglect of the excited-state contributions $v' \neq 0$ in Eq. (3). The density evolves according to Eq. (1b) with the ponderomotive force replaced by $\nabla^2 |E_0 + h_0(t)e_0(r, t)|^2$.

In Fig. 2 we show some typical results from the scalar model driven by a spatially uniform field E_0 at the plasma frequency ($\omega_0 = 0$). For a range of E_0 , a stable nucleation cycle is observed, with a complete cycle over the interval $0 < t < t_c$. We expect that in a turbulent environment of other such nucleation sites, the strict periodicity of this cycle will be lost, but at a given site there may be strong correlations over a few cycle times for strong ion acoustic damping. We can isolate the collapse events occurring at the spacetime points (\mathbf{x}_i, t_i) defined by local maxima of $|\mathbf{E}(\mathbf{x}, t)|^2$. The multievent spectrum is given by the sum over N_c events in the observation time;

$$\mathbf{E}(\mathbf{k}, \omega) = \sum \exp(i(\mathbf{k} \circ \mathbf{x}_i - \omega t_i)) \mathcal{E}_i(\mathbf{k}, \omega).$$

Even if the behavior of the single-event spectra $\mathcal{E}_i(k, \omega)$ is well approximated by the unique parameters of an isolated event, as modeled by the computations discussed above, the turbulent power spectrum $|\mathbf{E}(\mathbf{k}, \omega)|^2$ still depends in detail on the correlations between events. For example, if one assumes that all events are independent (uncorrelated) then the power spectrum reduces to its incoherent part $\sum |\mathcal{E}_i(\mathbf{k}, \omega)|^2 \equiv N_c \langle |\mathcal{E}(\mathbf{k}, \omega)|^2 \rangle$. A reali-

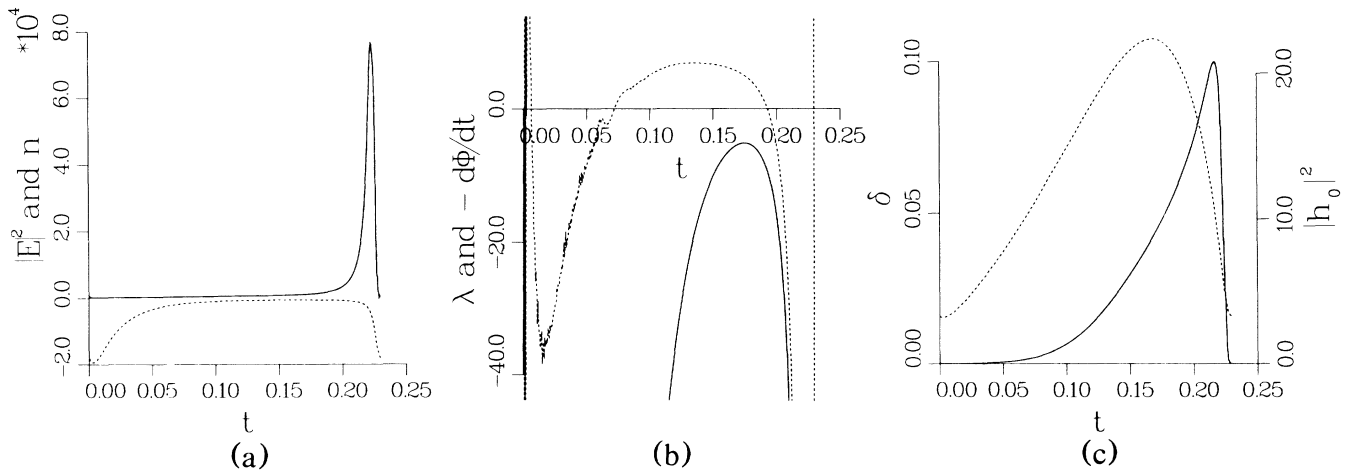


FIG. 2. Evolution of scalar caviton vs time for $E_0 = 5.0$, $m_i/m_e = 2 \times 10^4$, $v_i(k) = 0.9|k|$, $\omega_0 = 0$. (a) Values of $|E|^2$ (solid line) and n (dashed line) (at $r = 0$). (b) Lowest eigenvalue λ_0 (solid line) and phase velocity Φ_0 (dashed line); note the rapid decrease of λ_0 for $t \geq 0.20$ associated with collapse. (c) Amplitude $|h_0(t)|^2$, energy in ground state (solid line), and radius of collapsing state $\delta_0(t)$, defined as value of $r = \delta_0(t)$ which maximizes $r^2 |e_0(r, t)|^2$ (dashed line).

zation of $|\mathcal{E}_i(k, \omega)|^2$ for the scalar model is constructed by taking the temporal transform of the function $f(t) = h_0(t)e_0(k, t)$ for $0 < t < t_c$ and $f(t) = 0$ for $t_c < t < T$, where T is chosen to give the desired frequency resolution, and $e_0(k, t)$ is the spatial Fourier transform of $e_0(r, t)$. In Fig. 3 such spectra are displayed.

Spectral peaks result from a modulation of the spectrum with an (angular) frequency period $\Delta\omega \approx 2\pi/\Delta t_c$, where Δt_c is the caviton lifetime as measured by the width in time of the total electrostatic energy pulse as shown in Fig. 2. For ionospheric parameters¹² we estimate from our simulation that $\Delta t_c \leq 0.1$ ms. The k dependence in this model arises from the k dependence of $e_0(k, t)$; for a localized state for $k\delta_0 > 1$ we expect $e_0(k, t) \sim \delta_0^{p/2}(t)\exp[-k\delta_0(t)]$. For increasing k , smaller values of δ_0 are favored and these correspond to more tightly collapsed states with more negative frequencies.

Let us assume that the early-time spectrum from low-duty-cycle experiments⁹ can be identified with the *incoherent average* $\langle |\mathcal{E}(k, \omega)|^2 \rangle$ of single-event spectra. In this averaged spectrum the individual spectral peaks may be smeared out but it is reasonable to assume that the half-power frequency width is approximately that of the first and strongest maximum of the single-event spectra. Application of this argument to the data of Djuth, Gonzales, and Ierkić⁹ in this regime—e.g., their Fig. 4—leads also to a value $\Delta t_c \sim 0.1 \pm 0.05$ ms.

In the single-caviton-model calculations we find that the electric field $\mathcal{E}(k, t)$ is phase locked to the pump field with a relative phase which is insensitive to parameters such as E_0 and ω_0 . If the fluctuations in the single-event amplitudes $\mathcal{E}_i(k, t)$ are assumed to be small than we can write in the multicaviton case

$$|\mathbf{E}(\mathbf{k}, \omega)|^2 \approx |\rho(\mathbf{k}, \omega)|^2 \langle |\mathcal{E}(\mathbf{k}, \omega)|^2 \rangle,$$

where $\rho(\mathbf{k}, \omega) = \sum \exp[i(\mathbf{k} \cdot \mathbf{x}_i - \omega t_i)]$ is the transform of the spacetime density of caviton events. A possible

consequence of this observation is that the strong peaks in the observed incoherent scatter radar spectra, which develop after several ms in low-duty-cycle experiments,⁹ are the result of the development of a correlated state of spacetime events whose structure factor $|\rho(\mathbf{k}, \omega)|^2$ has sharp peaks. This correlation could arise from background density modulations, with wavelengths of a few meters, developing in a few ms, which sensitively modulate the nucleation process. These modulations might arise from background temperature fluctuations, not treated by the model of Eqs. (1), which are caused by strong local turbulent heating. A measure of this is ν_{eff} , the effective absorption of the pump, which is at least an order of magnitude greater than collisional absorption.¹

The observed^{13,14} altitude dependence of the plasma line for given k and ω is in accord with our model because localized states are not tied to the linear Langmuir wave dispersion relation. We estimate¹² that cavitons should be most strongly excited near the first Airy maximum of the heater, not at the lower altitude where the *linear*, photoelectron-enhanced Langmuir wave signal is observed. The model is also consistent with the maximum scale of density fluctuations inferred by Birkmayer, Hagfors, and Kofman¹⁴; cavitons for ionospheric parameters would have spatial dimensions in the range of 50–5 cm. In the simulations of Ref. 1 the spectrum $\langle |\mathbf{E}(\mathbf{k}, \omega)|^2 \rangle$ was nearly isotropic as a function of the direction of \mathbf{k} for $E_0 > 1.0$, $\nu_i = 0.9$; we find a similar isotropy¹² when the geometric field \mathbf{B}_0 is taken into account. This appears to be consistent with observations⁴ and contrasts with the weak-turbulence prediction¹⁵ of a ratio of about 10^{-4} between fluctuations with \mathbf{k} at 45° from \mathbf{B}_0 compared to \mathbf{k} parallel to \mathbf{B}_0 .

The Fourier transform to $\mathcal{E}(r, t)$ is given by

$$\mathcal{E}(k, \omega) \approx \int dt \exp\{i[\omega t + \Phi_0(t)]\} |h_0(t)| e_0(k, t),$$

where Φ_0 is the phase of $h_0(t)$. For large negative ω we

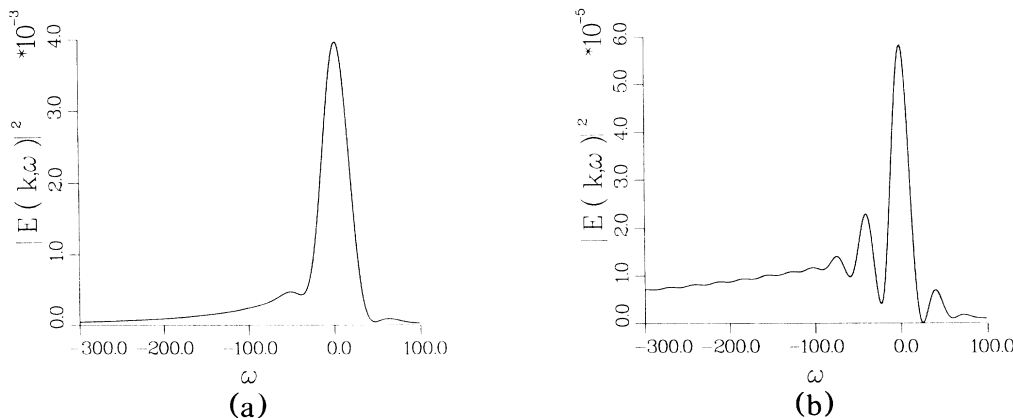


FIG. 3. $|E(k, \omega)|^2$ for the scalar model for parameters of Fig. 2; (a) spectrum of event in Fig. 2 for $k = 12.0$ and (b) spectrum of event in Fig. 2 for $k = 40.0$.

can make asymptotic estimates based on a stationary-phase evaluation of the time integral; the stationary-phase points $t=t_s$ occur approximately where $\omega = -\dot{\Phi}_0(t_s)$. From Fig. 2 we see that the ground state has large negative phase velocities where $\dot{\Phi}_0(t) \rightarrow -\lambda_0(t)$ as $t \rightarrow t_c$ and can satisfy the stationary-phase condition. In this temporal regime one comes closest to the self-similar scaling for the collapsing state $e_0(r,t) = \delta_0(t)^{-D/2} \Psi_0(r/\delta_0(t))$, with the spatial Fourier transform $e_0(k,t) = \delta_0(t)^{D/2} \int d\xi \exp(-ik\delta_0\xi) \Psi_0(\xi)$. The self-similar behavior is¹⁰ $\delta_0(t) \sim (t_c - t)^{2/D} \sim \lambda_0(t)^{-1/2}$, where t_c is the collapse time. Using these behaviors in the stationary-phase evaluation of the Fourier integral we find the asymptotic behavior $|E(k,\omega)|^2 \sim |\omega|^{-(1+3D/4)}$ as $\omega \rightarrow -\infty$. This asymptotic prediction is observed in the $D=2$ vector Zakharov simulations and in the scalar simulations to an accuracy of 10%.

Individual caviton spectra at a given spatial location within a caviton, $|\mathbf{E}(\mathbf{x},\omega)|^2$, could be measured in principle in experiments such as those of Wong and Cheung.¹⁶ Our calculations¹² show many of the same features as seen for $|\mathbf{E}(\mathbf{k},\omega)|^2$, including a modulation at $\Delta\omega = 2\pi/\Delta t_c$ and an asymptotic regime for large negative ω where $|\mathbf{E}(\mathbf{x},\omega)|^2 \sim |\omega|^{-(1-D/4)}$.

This strong turbulence model does not depend on linear parametric instabilities except perhaps for the initial excitation from quiescent conditions—a few ms in the ionosphere case—following the onset of heating. These instabilities are suppressed^{1,6} in the developed turbulent state which is sustained by the nucleation of localized states.

We wish to thank P. Y. Cheung, J. A. Fejer, T. A. Hagfors, D. R. Nicholson, and F. W. Perkins for helpful discussions. This work was supported by the U.S. Department of Energy and the Office of Naval Research.

¹David Russell, D. F. DuBois, and Harvey A. Rose, Phys. Rev. Lett. **60**, 581 (1988).

²V. E. Zakharov, Zh. Eksp. Teor. Fiz. **62**, 1745 (1972) [Sov. Phys. JETP **35**, 908 (1972)].

³For a comprehensive review and other references see J. A. Frejer, Rev. Geophys. Space Phys. **17**, 135 (1979); J. A. Frejer, C. A. Gonzales, H. M. Ierkić, M. P. Sulzer, C. A. Tepley, L. M. Duncan, F. T. Djuth, S. Ganguly, and W. E. Gordon, J. Atmos. Terr. Phys. **47**, 1165 (1985). Note that for $\omega \ll \bar{\omega}_p$ the spectrum for the envelope field \bar{E} (in physical units

denoted by tildes) is related to that of the high-frequency electron density fluctuations, which is observed in incoherent scatter radar measurements, through Poisson's equation which gives

$$|\tilde{n}_e(\bar{\mathbf{k}}, \omega_{pe} + \bar{\omega})|^2 n_0^{-2} = \frac{1}{4} (\tilde{k} \lambda_{De})^2 |\tilde{\mathbf{E}}(\bar{\mathbf{k}}, \bar{\omega})|^2 (4\pi n_0 T_e)^{-1}.$$

⁴J. P. Sheerin and D. R. Nicholson, Phys. Lett. **97A**, 395 (1983). These authors estimated the radar cross section for "solitons" (our cavitons) but did not compute the spectral shape.

⁵The units of time, distance, electric field, and density fluctuations are respectively: $\frac{3}{2} (m_i/m_e) \omega_{pe}^{-1}$, $\frac{3}{2} (m_i/m_e)^{1/2} \lambda_{De}$, $8(\pi n_0 T_e m_e / 3 m_i)^{1/2}$, and $n_0 (4 m_e / 3 m_i)$. Frequencies in the envelope representation are measured relative to the mean ω_{pe} . Thus our dimensionless drive frequency ω_0 is related to the absolute dimensional drive frequency $\bar{\omega}_0$ by $\omega_0 = \frac{3}{2} (m_i/m_e) (\bar{\omega}_0 / \omega_{pe} - 1)$.

⁶G. D. Doolen, D. F. DuBois, and H. A. Rose, Phys. Rev. Lett. **54**, 804 (1985); D. Russell, D. F. DuBois, and H. A. Rose, Phys. Rev. Lett. **56**, 838 (1986).

⁷These simulations correspond to the case in Fig. 4(a) of Ref. 1 where a marginally developed inertial range in k_x was observed.

⁸The criterion for a localized state may not be $\bar{\omega} < 0$ [or in the context of Eq. (2), $\lambda_v < 0$] but rather $\omega < \lambda_{loc}$, where $\lambda_{loc} > 0$ is due to the random environment of density fluctuations of a particular localized state. This is consistent with simulations, not reported here, where the drive frequency $\omega_0 > 0$.

⁹A. Y. Wong, G. J. Morales, D. Eggleston, J. Santoru, and R. Behnke, Phys. Rev. Lett. **47**, 1340 (1981); F. T. Djuth, C. A. Gonzales, and H. M. Ierkić, J. Geophys. Res. **91**, 12089 (1986).

¹⁰A. A. Galeev, R. Z. Sagdeev, Yu. S. Sigov, V. D. Shapiro, and V. I. Shevchenko, Fiz. Plazmy **1**, 10 (1975) [Sov. J. Plasma Phys. **1**, 5 (1975)]; A. A. Galeev, R. Z. Sagdeev, V. D. Shapiro, and V. I. Shevchenko, Pis'ma Zh. Eksp. Fiz. **24**, 23 (1976) [JETP Lett. **24**, 21 (1977)].

¹¹The scalar equations have the same form as Eqs. (1) with $\mathbf{E}(\mathbf{x},t)$ and \mathbf{E}_0 replaced by $E(r,t)$ and E_0 and with the divergence operator on both sides of Eq. (1a) dropped.

¹²D. F. DuBois, H. A. Rose, and D. A. Russell, to be published.

¹³D. B. Muldrew and R. L. Showen, J. Geophys. Res. **82**, 4793 (1977).

¹⁴W. Birkmayer, T. Hagfors, and W. Kofman, Phys. Rev. Lett. **57**, 1008 (1986).

¹⁵J. A. Fejer and Y. Y. Kuo, AGARD Conf. Proc. **138**, 11 (1973); F. W. Perkins, C. Obermand, and E. J. Valeo, J. Geophys. Res. **79**, 789 (1974).

¹⁶A. Y. Wong and P. Y. Cheung, Phys. Rev. Lett. **52**, 1222 (1984).